Biomass and Bioenergy 151 (2021) 106123

Contents lists available at ScienceDirect

Biomass and Bioenergy

journal homepage: www.elsevier.com/locate/biombioe

Modeling of cost optimized process integration of HTL fuel production

Christina Penke *, Leonard Moser, Valentin Batteiger

Bauhaus Luftfahrt e. V., Willy-Messerschmitt-Str. 1, 82024, Taufkirchen, Germany

ARTICLE INFO

Keywords:
Hydrothermal liquefaction (HTL)
Liquid biofuel
Integration
Modeling
Sustainable aviation fuel
Sewage sludge

ABSTRACT

Hydrothermal liquefaction (HTL) is an advanced biomass conversion process for biocrude production from a broad variety of organic feedstock, including wet waste streams. The intermediate biocrudes can be further upgraded to liquid hydrocarbon fuels and thereby contribute to the mitigation of greenhouse gases from the transport sector. This work investigates an optimized sub-system integration of transportation fuel production via sub-critical HTL of primary sewage sludge. The plant design integrates HTL conversion, biocrude upgrading via hydrotreatment, and an energetic valorization of the residual aqueous phase from HTL conversion via catalytic hydrothermal gasification (cHTG). The option of on-site hydrogen production via reforming of cHTG gas is examined for the purpose of biocrude upgrading. The modeling results show that the hydrogen demand for hydrotreatment could be covered by the valorization of the HTL by-products. The thermal management of an integrated biofuel plant is optimized with respect to subsystem cost based on in-depth process modeling to quantify mass and energy flows and principles of pinch analysis to design a heat exchanger network. The cost optimized configuration results in an overall process energy efficiency of 40.5%. The results provide a basis for design choices for future HTL plants.

1. Introduction

HTL receives increasing attention in research and development as a highly versatile process that can convert a broad range of organic feedstock. The HTL process might represent a competitive alternative to other renewable fuel production processes, due to its promising ecological and economic performance [1,2]. In HTL, biomass is converted at temperatures of 300–420 °C and pressures of 15–35 MPa into a highly viscous bio-oil, commonly referred to as biocrude [3,4]. This intermediate biocrude can be further upgraded to liquid hydrocarbon fuels via catalytic hydrotreatment. Additionally the HTL process produces solids, a gas phase containing mainly CO_2 and an aqueous phase consisting mainly of water and water-soluble components [5].

The application of hydrothermal process conditions has long been studied to produce liquid fuels from biomass. Already in the 1980s, a hydrothermal process called HTU (hydrothermal upgrading) was developed by Shell laboratories in the Netherlands [6]. A pilot plant was set up to demonstrate biocrude production from woody biomass without using a catalyst. In contrast, the CatLiq Process, developed in the early 2000s, uses heterogeneous (ZrO_2) or homogeneous catalysts (e.g., K^+, CO^{2-}_3, OH^-) to produce an energy-rich bio-oil from wet biomass [7].

However, most of the studies that have been published recently focus on HTL. The by far larger part rely on batch-mode experiments. Batch HTL experiments allow for fast screenings of a broad range of process conditions, e.g. to identify suitable operating points for continuous systems or to analyse involved chemical reaction schemes and the impact on process conditions on the product phases.

However, batch-mode operation of an HTL process is less suitable for industrial application, where efficient heat recovery and high throughput is required to enable an economically reasonable process chain, particularly if targeting commodities like fuels as main products. Therefore, it is of great importance, that continuous-mode HTL facilities are established and operated by both research institutes and companies that enable experiments in an industrially relevant environment.

The pilot-scale HTL plant operated by Aarhus University allows for a throughput (approximately 60–100 L h^{-1}) with typical dry matter content of 0.2 and enables testing at industrially relevant process conditions with integrated heat recovery [3]. This throughput corresponds to a power equivalent of up to 90 kW considering wood as HTL feedstock.

While most of the existing continuous-mode HTL plants are operated in subcritical (often near-critical) regimes, there is also significant interest in super-critical HTL systems. Important work in this field has been conducted by Aalborg University [8] and Steeper Energy [9].

* Corresponding author.
E-mail address: Christina.penke@bauhaus-luftfahrt.net (C. Penke).

https://doi.org/10.1016/j.biombioe.2021.106123
Received 8 November 2020; Received in revised form 2 May 2021; Accepted 16 May 2021
Available online 6 June 2021
0961-9534/

Supercritical HTL offers the potential of improved biocrude quality and faster kinetics, but is associated with technical challenges resulting from increased temperatures and pressures compared to subcritical conditions. While the HTL system of Aarhus University is typically operated at 350 °C and 22 MPa for example, Steeper Energy's Hydrofaction™ is operated at 390–420 °C and 30–35 MPa [10]. A detailed review of reported continuous HTL plants can be found in a publication by Castello et al. [11].

Hydrothermal liquefaction has not been commercially implemented yet and can therefore still be considered as emerging technology. However, there are and have been several projects by companies aiming industrial deployment and commercialization of HTL-based production processes. Australia-based company Licella has developed the Cat-HTR™ (Catalytic Hydrothermal Reactor) process. Licella operates three separate pilot plants in Somersby, NSW, Australia. The first generation pilot plant was built in 2009 with a capacity of 100 tonnes per year. The second and third generation pilot plants were built in 2011 and 2012, respectively and are able to process 1000 and 10,000 tonnes per year of organic matter, respectively. The fourth generation commercial plant was planned to be commencing in 2019 with no capacity indication yet [12]. Another Australien company, Muradel, had developed a HTL-based technology platform (Green2Black™) that was demonstrated in a pilot plant with a capacity of 3000 L feed slurry per day. The slurry was delivered by Muradel's microalgae cultivation facility. Next to microalgae, the company has also applied end-of-life car tires and sewage sludge [13].

In comparison to other biofuel conversion technologies, HTL is particularly favorable for the conversion of biomasses that are readily available in aqueous slurries, e.g. sewage sludge, manure or microalgae. An energy intensive drying step can be avoided in many cases as water serves as reaction medium (solvent) and reactant. The hydrothermal processing of waste materials represents a disposal process in addition to the fuel production, which can contribute to the plant economics.

Sewage sludge represents an example of an aqueous waste that is available at negative costs in many places [14] and thus is an attractive feedstock for HTL. However, the processing of sewage sludge also involves technical challenges that need to be solved. The composition of sewage sludge can vary significantly [,16]. When designing a HTL plant, this must be taken into account, since the composition of the feedstock has a major impact on process performance parameters, e.g., yield and quality of biocrude as well as other product phases and energy efficiency. When sewage sludge is used as HTL feedstock the biocrude usually contains a high share of mineral components and heteroatoms [17], which pose a challenge for biocrude upgrading and compliance of the final product with transportation fuel specifications.

So far, only a limited number of studies have been devoted to upgrading of HTL biocrude. A small number of reviews of research conducted in this field can be found in literature [11,18,19].

The majority of upgrading studies of HTL biocrudes are based on batch-mode experiments that do not represent an industrially relevant environment, while only very few reported studies are based on upgrading in continuous mode.

A team from PNNL introduced a bench-scale hydroprocessing system using a molybdenum sulfide catalyst for the upgrading of microalgae derived biocrude [2,20]. Results show that oxygen, nitrogen and sulfur compounds could be reduced significantly. Another study dealing with batch reactor upgrading was recently published by Haider et al. [21]. Two highly nitrogenous biocrudes obtained from primary sewage sludge and spirulina biomass were investigated therein. Due to the lack of thermal stability of the raw biocrudes at the severe conditions (~400 °C) required for appropriate hydrodenitrogenation, a two-stage approach was conducted. A first, low-temperature stabilization stage was used to prepare biocrude for a second stage of upgrading under more severe conditions. This approach yielded in complete deoxygenation and removal of 92% of nitrogen for both biocrudes, while simultaneously reducing the coke formation from 9.1% to 3.4%–1.0% and 0.7% for spirulina and sewage sludge, respectively [21].

Commercial implementation of a HTL process needs a preferably complete conversion of carbon-containing compounds into fuels. However, the aqueous phase that is formed during HTL conversion can contain more than 0.50 kg kg^{-1} of the carbon originally present in the feedstock, with a total organic carbon value of 15–50 g L^{-1} [22]. Application of catalytic hydrothermal gasification (cHTG) represents a promising option to transform the organic content of the aqueous phase into a combustible gas [23].

The product gas can be used for on-site heat and power generation. In the case of sufficiently high product gas quantities, it can be considered to process the residual raw gas by means of gas scrubbing and sell methane on the market. Besides that, the combination of HTL and cHTG brings several additional benefits. cHTG simplifies subsequent aqueous phase treatment, as potentially toxic organic components are removed by conversion into useful products. Furthermore, methane from cHTG gas provides an on-site resource for producing H_2 via steam reforming. H_2 is required subsequently for biocrude upgrading. The proposed HTL process chain is schematically depicted in Fig. 1.

In order to optimally dimension the individual process steps, modeling of the entire process chain is required. This issue is addressed by an in-depth modeling of all individual process steps using Aspen Plus. Along this process chain, the most important reaction pathways are identified and mapped in order to provide accurate information about product yields and compositions. The model is based on thermodynamic and reaction kinetic data, and validated with experimental data, which allows comprehensive statements on mass and energy balances as well as statements regarding the composition of different products. In order to optimally arrange and dimension heat exchangers, a cost optimization of the HTL process is performed and the expected savings in heat demand are assessed. It is shown that effective heat recovery is key for cost-competitive and environmentally friendly fuel production. Energy demand can be significantly reduced with the use of a heat management system covering the entire process. This study addresses the research gap of the process integration of individual sub processes in an entire HTL process chain and the associated challenges in thermal management. This study was carried out as part of the EU project HyFlexFuel [24] and results of this study were previously published in a contribution at virtual EUBCE 2020 [25].

2. Materials and methods

In order to depict a HTL process chain using sewage sludge as accurately as possible, experimental results generated by pilot-scale plants were used [4,26]. With additional consideration of reaction mechanisms and thermodynamic data, mass and energy balances for fuel production were developed. The integrated HTL process chain is upscaled to a biocrude production of 10,000 tonnes per year according to biomass potentials assessed by Horschig et al. in a catchment area of 50 km [27]. For simplification reasons, the energy demand for all pumps transporting liquids or slurry was modeled to be 12 Wh L^{-1}.

2.1. Feedstock

Primary sewage sludge representing a wet waste stream is considered as feedstock (FS) in this study. Sewage sludge is typically provided as slurry ready to be used in HTL (with possibly prior adjustment of dry matter content). In this model the chemical composition of sewage sludge is represented by four basic biochemical groups, namely lipids, carbohydrates, proteins and lignin. Table 1 shows the relative abundance of these components as well as the considered ash content in the feedstock. The modeling was carried out with a dry matter (DM) mass fraction of 0.20, which still allows pumping, facilitates high yields and energy efficiency and largely avoids coke formation [5].

In the simulation, 32 model compounds are generated representing the four biochemical groups by the formation of typical hydrolysis

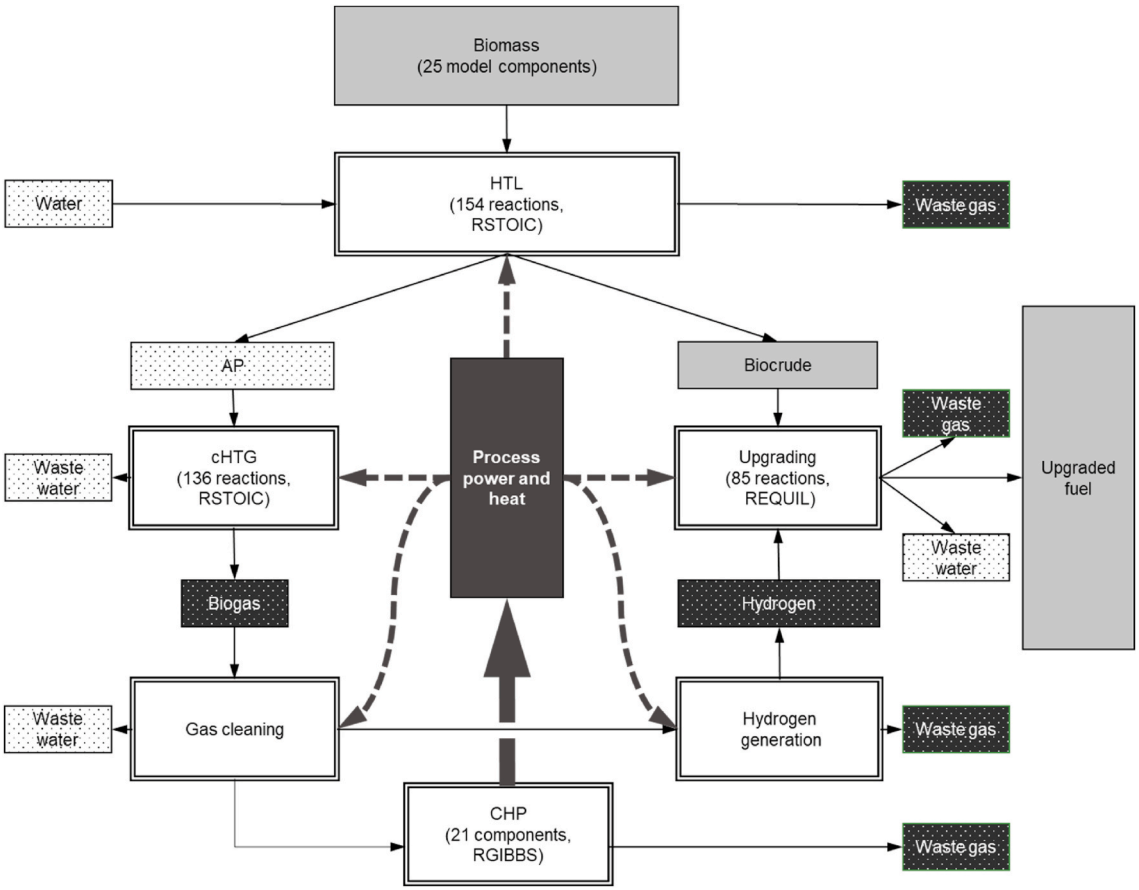

Fig. 1. Process overview of the modeled and optimized HTL production chain (AP: aqueous phase; cHTG: catalytic hydrothermal liquefaction; CHP: combined power and heat plant). As reactor models RSTOIC, REQUIL and RGIBBS were used.

Table 1
Biochemical composition of sewage sludge.

Biochemical group	Mass fraction [−]
Lipid	0.039
Carbohydrate	0.450
Protein	0.233
Lignin	0.073
Ash	0.205

products, as well as the ash fraction. It is assumed that the ash fraction is not effected by hydrolysis conditions and is therefore not involved in the simulation as a reaction partner. Databases containing thermodynamic and reaction kinetic data are available for most model compounds in the software Aspen Plus v10 [22]. It should be noted that four amino acids, namely cystein, histidine, proline and arginine could not be modeled directly, due to missing parameters in the databases. Instead of the actual amino acids, the following alternative compounds 3-mercapto-propionic acid, 2-ethylimidazol, pyrrolidine and valeric acid were used, respectively. The missing nitrogen content was compensated by an additional amount of ammonia. Table 1 quantifies the assumed feedstock composition and Fig. 2 shows the formation of exemplary model compounds from the four considered biochemical groups via hydrolysis.

A detailed list of all model components used for the feedstock can be found in the appendix (Table A1).

2.2. Thermochemical modeling of the reactions

HTL and cHTG reactors are modeled using RSTOIC reactor model and Soave-Redlich-Kwong (SRK) equation of state as property method. Peng-Robinson equation of state with Boston-Matthias modification (PR-BM) was used as property method for biocrude upgrading. The HT reactor is modeled by a REQUIL reactor model. Table 2 gives an overview of the reactor models and the number of chemical compounds or reactions considered.

Based on literature [28–31], typical HTL reactions and biocrude compounds were identified and integrated in the Aspen model. The fractional conversions of the reactions in the HTL RSTOIC reactor are adjusted according to the elemental analyses and experimental product yields. In the case of the cHTG RSTOIC reactor, the fractional conversion of the reactions can be considered as the efficiency of the cHTG process. The model assumes that all reactions occur with equal likelihood, a fractional conversion or efficiency of 99% is considered.

Depending on the pH, a considerable amount of CO_2 is dissolved as CO_3^{2-}, especially under higher pressures. Since the equilibrium between gaseous CO_2 and dissolved CO_3^{2-} is not modeled, the assumption is made that 35% of gaseous CO_2 is dissolves in the aqueous phase according to Zhu et al. [32].

References for the modeling are experimental measurements performed at the HTL pilot plant at Aarhus University [3], the gasification pilot plant at Paul Scherrer Institute [33] and the continuous biocrude upgrading unit at Aalborg University [34].

2.3. Process modeling

2.3.1. Hydrothermal liquefaction

The feed slurry is heated and enters the HTL reactor (building block RSTOIC) at a temperature of 350 °C and a pressure of 22 MPa. This means that the HTL reactor is operated under sub-critical conditions. The gas resulting from the biomass conversion, consisting mainly of

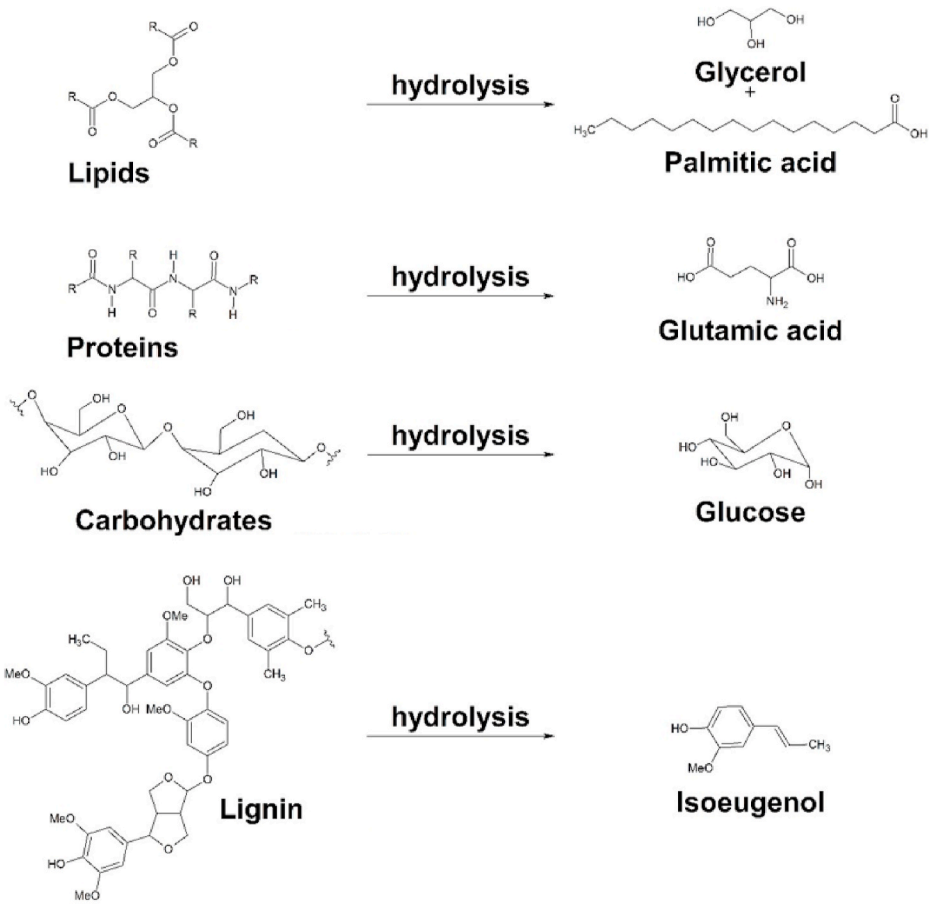

Fig. 2. Exemplary hydrolysis reactions of four biochemical groups for the modeling of HTL of sewage sludge in Aspen Plus.

Table 2
Considered model options for the different process steps using Aspen Plus (RSTOIC: Stoichiometric reactor model, RGIBBS: Gibbs reactor model, REQUIL: Equilibrium reactor model).

Process step	Reactor model	Number of defined reactions or compounds
HTL	RSTOIC	154 reactions
Upgrading	REQUIL	85 reactions
cHTG	RSTOIC	136 reactions
CHP	RGIBBS	21 compounds

CO_2, is discharged, while the remaining product mixture is cooled to a temperature of 80 °C at ambient pressure and separated into biocrude, aqueous phase and a solid residue applying a gravimetric phase separation. The phase separation processes are modeled by using different building blocks in Aspen. SEP2 unit block with operating conditions of 0.2 MPa and 100 °C was chosen for solid separation while SEP unit block with operating conditions of 0.1 MPa and 80 °C was selected for modeling the gas separation. In order to separate the two liquid HTL phases (aqueous phase and biocrude) a decanter unit block with operating conditions of 0.1 MPa and 80 °C is used in the simulation. In order to match the experimental mass flows of the biocrude and the water phase as well as the elemental analysis of the biocrude, the separation efficiency of several components is adjusted. After separation, the aqueous phase possesses a total organic carbon (TOC) of 43.5 g L^{-1} and has therefore to be treated with a membrane separator in order to upconcentrate the TOC. The membrane separator was modeled using a SEP2 unit block at 0.1 MPa and 80 °C. It is assumed that the TOC is increased to 80 g L^{-1}. A detailed flowchart of the modeled HTL process including the phase separation and the upconcentration of the aqueous phase is shown in Fig. 3.

2.3.2. Hydrotreating

The hydrotreating of the biocrude was modeled by using an REQUIL reactor unit block operated at 7 MPa and 400 °C with a hydrogen surplus of 23.2 mol per kilogram of biocrude according to Tzanetis et al. [35]. Subsequently the upgraded biocrude stream is cooled, depressurized and separated. A gaseous phase (refinery gas) is separated by a SEP unit block operated at 50 °C and 5 MPa. It is assumed that remaining hydrogen in the refinery gas is recycled and made available again for upgrading. The liquid phase is subsequently cooled, depressurized and separated into the upgraded biocrude and a wastewater stream by a decanter unit block operated at 0.1 MPa and 25 °C.

2.3.3. Catalytic hydrothermal gasification

For modeling the catalytic hydrothermal gasification process an RSTOIC reactor is used at super-critical operating conditions of 450 °C and 28 MPa. The fractional conversion of all reactions is assumed to be 99%. The reactor stream is subsequently cooled, depressurized and separated. For separation of the liquid wastewater and the gas phase a SEP unit block operated at 1 MPa and 80 °C is used. A gas treatment process for accumulation of the methane is included in the model. It is assumed that 0.41 kg of methane can be produced from 1.00 kg of raw biogas related to an energy demand of 155 kJ.

2.3.4. Use of methane

Two options of dealing with the methane produced by cHTG and subsequent gas treatment are assessed. One option represents a steam reforming process conducted at a temperature of 800 °C and a pressure of 2 MPa to produce on-site hydrogen that is required for the

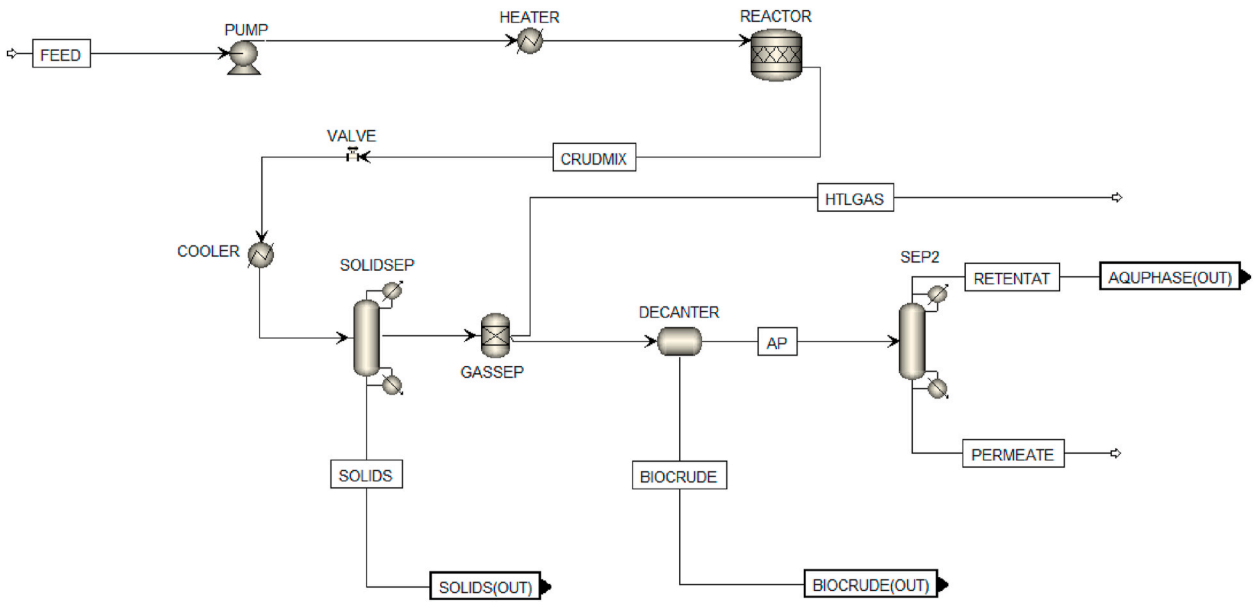

Fig. 3. Flowsheet diagram of all hydrothermal liquefaction process steps modeled in Aspen Plus.

hydrotreating process step. The other option is an energetic use of methane to cover the heat demand of an HTL production chain. Combustion of methane was modeled in Aspen Plus using the RGIBBS reactor model. The exhaust gas (~800 °C) of the combustion is used for heat recovery. Furthermore, a combination of both options is investigated by varying the share of application of combined heat and power (CHP) and hydrogen generation.

2.4. Heat exchanger network

The required hot and cold demands for the individual process steps are evaluated using Aspen Plus. In order to achieve the best energetic option for the arrangement of heat exchangers, process integration was performed using principles of pinch analysis in Aspen Energy Analyzer v10. For ΔT_{min} a value of 5 °C was assumed in the modeling.Counter current shortcut recuperators are used as heat exchangers. The heat exchanger surface area A is derived from the following correlation

$$\mathrm{Q} = \mathrm{UA}\Delta\mathrm{T_{LM}} \tag{1}$$

where Q corresponds to the heat flow in the heat exchanger. The overall heat transfer coefficient U is assumed to be 15 W m^{-2} K^{-1} for all heat exchangers. The logarithmic mean temperature difference ΔT_{LM} represents the driving force for the heat exchange between process streams and is given by

$$\Delta\mathrm{T_{LM}} = \frac{\Delta\mathrm{T_1} - \Delta\mathrm{T_2}}{\ln\left(\frac{\Delta\mathrm{T_1}}{\Delta\mathrm{T_2}}\right)} \tag{2}$$

where $\Delta T1$ corresponds to the temperature difference of the hot stream, $\Delta T2$ to the temperature difference of the cold stream. Two references for process optimization are taken into account. For comparison, "No HR" describes a hypothetical HTL process chain where no heat recovery (HR) is applied. For "sep HR" it is assumed that there is internal heat recovery in the individual sub-processes considered with a recovery rate of 80%. "HEN" considers a fully integrated heat recovery.

2.5. Cost modeling

The optimization minimizes the overall production costs of an integrated HTL process. Based on the computed mass and energy balances, the operating costs and the achievable profits of a HTL production are estimated. The assumed costs for feedstock and energy supply as well as the expected revenues from sales of the HTL products are shown in Table 3.

As a reference for the capital expenditures (CAPEX) of the plants for biocrude production, gasification, hydrotreating and hydrogen supply serves a study from PNNL, describing a preliminary TEA of a HTL fuel production [15,16,36]. The costs of heat exchangers are estimated according to Keshavarzian et al. with 3000 € m^{-2} [37]. Economy of scale is considered by using the following equation in relation to the quotient of new (Q_n) and reference capacity (Q_r) for the calculation of the present value (PV)

$$\mathrm{PV_{Scale}} = \mathrm{PV}\left(\frac{\mathrm{Q_n}}{\mathrm{Q_r}}\right)^{\mathrm{m}}. \tag{3}$$

The correlation exponent m is derived from the cost of large (C_l) and small facilities (C_s) as well as the capacity of large (Q_l) and small facilities (Q_s)

$$\mathrm{m} = \frac{\log\mathrm{C_l} - \log\mathrm{C_s}}{\log\mathrm{Q_l} - \log\mathrm{Q_s}}. \tag{4}$$

The lifetime of the HTL plant is assumed to be a period of 10 years and is taken into account by annualization of the investment costs using $LCOE$ (levelized cost of energy) methodology

$$\mathrm{LCOE} = \frac{I + PV}{F \cdot A}. \tag{5}$$

I represents the upfront investment costs, PV is the present value of the operational costs accumulated over the lifetime, F is the annual amount of fuel produced by an HTL plant, and A denotes the annuity factor

Table 3
Considered operating and investment costs for fuel production by HTL.

	Cost	Ref.
Energy supply	77 € $(MWh)^{-1}$	[42]
Waste water treatment	1.77 € m^{-3}	[43]
Gas treatment	0.10 € m^{-3}	[44]
CAPEX CHP (microturbine)	1000 € $(kWh)^{-1}$	[45]
CAPEX HEX	3000 € m^{-2}	[37]
Methane	0.40 € kg^{-1}	[46]

$$A = \frac{1-(1+i)^{-n}}{i}. \quad (6)$$

For the calculation of annuity factor *A*, *i* denotes the interest rate and *n* the lifetime of the plant. An interest rate *i* of 6% per year is considered in the calculations. Furthermore, it is assumed that labor cost, revenues from sewage sludge disposal and from the fuel products (naphtha, kerosene, diesel) are equal for all considered process configuration and can therefore be excluded from the cost optimization.

2.6. Assessment of process performance

Since biocrude is the primary target product in the HTL process, biocrude yield Y_{bc} is often used as central metric to improve the plant economics. The biocrude yield is expressed as the mass ratio of the obtained biocrude ($m_{bc,dry}$) to the feedstock input ($m_{FS,dry}$)

$$Y_{bc} = \frac{m_{bc,\ dry}}{m_{FS,\ dry}} \quad (7)$$

However, the metric yield of biocrude neglects the quality of the yielded products. The product quality is reflected, e.g., in their specific energy, typically measured as higher heating value (HHV). The HHVs of the feedstock and the biocrude are calculated according to the equation proposed by Milne et al. [38] based on elemental composition and ash content (element and ash fraction in %; HHV_{Milne} in MJ kg^{-1}).

$$HHV_{Milne} = 0.341\ C + 1.322\ H - 0.12\ O - 0.12\ N + 0.0686\ S - 0.0153\ ash \quad (8)$$

Since the entire HTL process chain is considered, the fuel yield Y_{fuel} is determined using the following equation considering the obtained mass of fuel ($m_{fuel,dry}$)

$$Y_{fuel} = \frac{m_{fuel,\ dry}}{m_{FS,\ dry}}. \quad (9)$$

The process efficiency η of a HTL process is defined as the ratio of the energy output of the upgraded biocrude (in the following referred as fuel) and the sum of the energy content of the feedstock, the required electrical power P_{el} and the process heat H

$$\eta = \frac{HHV_{fuel} \cdot m_{fuel}}{HHV_{FS} \cdot m_{FS} + P_{el} + H} \quad (10)$$

3. Results

3.1. Elemental compositions

Elemental analyses (EA) of the product streams are used to validate the model of the HTL process chain. The comparison of the calculated elemental composition of feedstock, biocrude and upgraded biocrude with the respective results from literature values is shown in Fig. 4.

Keeping in mind that literature values can differ quite significantly, the calculated model values of the elemental analysis are in reasonable agreement to the references. According to the experimental results, the modeling clearly shows that an energetic upgrading of sewage sludge takes place. The relative carbon content can be increased by 59.6% during biocrude production, while an additional upgrading process leads to an increase of 85.6%.

The portion of heteroatoms can be reduced significantly during HTL processing and the subsequent upgrading process. The modeled upgraded biocrude shows nitrogen contents of 0.56 kg kg^{-1} and oxygen contents of 0.28 kg kg^{-1}. The sulfur content in the upgraded biocrude was modeled at 0.006 kg kg^{-1}. Both oxygen and nitrogen contents are slightly higher in the model compared to the experimental values of 0.2 kg kg^{-1} and 0.3 kg kg^{-1}, respectively. Nevertheless, a reasonable agreement can be stated. Looking at the deoxygenation and nitrogenation values during hydrotreatment, the results of EA can be fortified. The relative amount of removed oxygen amounts to 96.6%, while for denitrogenation the value is at 95.7%.

3.2. Simulated distillation

In order to estimate which amounts of final products can be expected from a distillation of the upgraded biocrude, the individual components of the upgraded biocrude were grouped according to their boiling points. Plotting of the cumulated masses of the individual components of the modeled upgraded biocrude over their respective boiling points leads to a simulated distillation curve, which is shown in Fig. 5. The calculated boiling point distribution is compared with experimental results obtained from literature.

As can be seen in Fig. 5, the overall distribution of masses fits quite well. Most significant differences can be observed in the temperature ranges of 28 °C–150 °C, 200 °C–275 °C and at temperatures above 450 °C. Nevertheless, the amounts of obtained product fractions are in an acceptable range compared to the experimental results, since simulated distillation curves can vary significantly when applying different conditions during hydrothermal liquefaction and hydrotreating. Also, it should be noted that the herein cited experimental results do not stem from a continuously operated process chain, but rather from different individual experiments that are not directly associated with each other. Therefore, experimental results should more be viewed as indication for the validation of the model, not as strictly needed match. The boiling point ranges of the product groups naphtha (28–150 °C), kerosene (150–250 °C) and diesel (250–350 °C) serve to determine the fuel product quantities that can be processed from upgraded biocrude. Thus, 0.218 kg naphtha, 0.196 kg kerosene and 0.466 kg diesel can be produced from 1.00 kg upgraded biocrude. Relative deviations from the literature values are in the range of 3.7% for naphtha, 11.7% for kerosene and 6.5% for diesel [39].

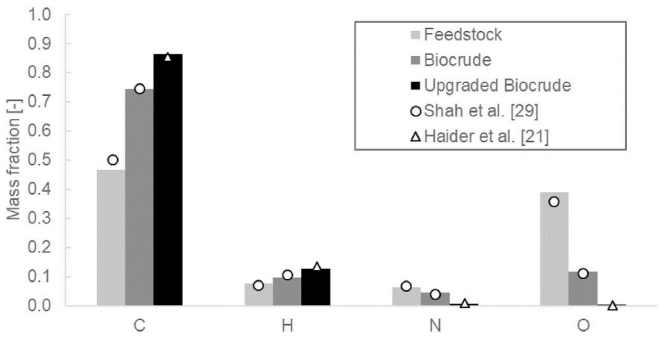

Fig. 4. Composition of feedstock, biocrude and upgraded biocrude using sewage sludge as HTL feedstock [29,47].

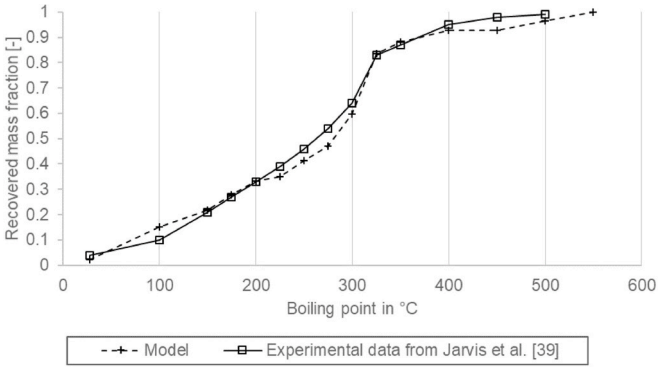

Fig. 5. Comparison of simulated distillation curves from upgraded biocrude of sewage sludge [39].

3.3. Use of methane from cHTG for CHP vs. hydrogen production

The gas produced by the catalytic gasification process is rich in methane (0.527 kg kg^{-1}) and has a HHV of 23.2 MJ kg^{-1}. By means of a gas purification process (e.g. by pressure swing adsorption) and a reduction of the other gas components such as CO_2 and NH_3, highly concentrated biomethane can be obtained. In the model, it was assumed that pure methane is present after gas purification. On the one hand, methane can be used on-site for the production of hydrogen via steam reforming. On the other hand, an energetic use of methane can generate process heat needed at different positions in the process. Fig. 6 shows the process efficiency as well as considered production costs for HTL fuel production using different shares of methane for on-site hydrogen production and CHP.

If methane is used completely for heat supply, the process efficiency is 44.6%, for a complete steam reforming of the methane the process efficiency amounts to 43.3%. These results can be explained by the fact that the process efficiency relates the energy resources used (biomass, heat, electricity) to the useable energy content in the upgraded fuel (see Equation (10)). The hydrogen demand is not considered in this efficiency calculation. A purely energetic use of methane is associated with higher sales revenues than a pure use of methane for hydrogen production. The bend in the cost graph at a mass ratio of 0.33 corresponds to a condition where the complete hydrogen demand of the system is covered, surplus produced hydrogen does not further improve the process efficiency.

3.4. Mass and energy balance

Based on the modeling, mass and energy balances are calculated covering the entire HTL process chain for the application of sewage sludge. The mass and energy balance for a HTL process with an on-site use of methane of 33% is shown in Fig. 7. Looking at the mass balance, it becomes clear that large amounts of aqueous phase are produced in addition to the desired biocrude, which corresponds to 24.9% based on the DM input. The model shows that 45.4% of the DM input, which corresponds to 45.8% of the initial carbon, ends up in the HTL aqueous phase. This underlines the high relevance of a treatment of the aqueous phase in a HTL process chain. cHTG has proved to be a suitable process for processing of aqueous HTL phases. For cHTG it is beneficial to increase the carbon concentration of the aqueous phase. It is computed that 78.0% of the initial carbon mass in the aqueous phase can be transferred into an upconcentrated aqueous phase (retentate) through membrane upconcentration. Thereby, the total organic carbon (TOC) of the aqueous phase is increased to a TOC of 96.8 g L^{-1} as feed for cHTG. The amount of carbon in the cHTG gas stemming from methane corresponds to 18.6% of the initial mass of carbon in the feedstock. Using the herein described setup, treatment of the aqueous phase is further facilitated, since large parts of the salts are concentrated in the brine phase and the organic content in the cHTG wastewater is reduced considerably. The estimations suggest that it is sufficient to use 33% of the purified biogas to cover the hydrogen demand in the biocrude hydrotreating process. The remaining gas can be used in a CHP unit to cover the electricity and heat demand for the HTL process chain.

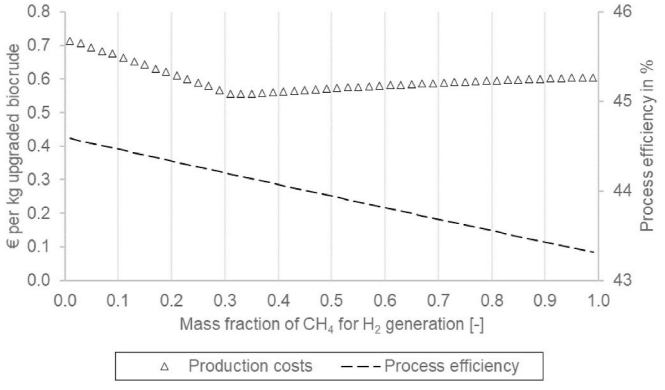

Fig. 6. Sales revenue and process efficiency of an HTL fuel production depending on the methane use for hydrogen generation or CHP.

The biocrude contains 51.6% of the initial carbon in the sewage sludge. Subsequent hydrotreatment of the biocrude yields an amount of 70.8% of upgraded biocrude based on the biocrude mass. Compared to the initial feedstock input, this corresponds to 18.6%. Considering the carbon mass flows, the yield of carbon in the upgraded biocrude (82.3%) based on the carbon content of the biocrude is even higher. This correlates to a total yield of 42.4% of carbon in the upgraded biocrude compared to the initial feedstock input. The mole flow of hydrogen input during hydrotreatment corresponds to a ratio of 23.2 mol per kilogram of biocrude. Based on the output of excess hydrogen, an actual hydrogen consumption of 22.9 g of H_2 per kilogram of biocrude was modeled.

The energy balance is derived from the mass flows of the overall HTL process chain, enthalpy flows associated with the heating and cooling demand as well as specific energy requirements of pumps, compressors and turbines. According to Milne et al. the HHVs are 17.02 MJ kg^{-1} for the sewage sludge, 36.83 MJ kg^{-1} for the biocrude and 45.73 MJ kg^{-1} for the upgraded biocrude.

For the energy balance the assumption was made that the sub processes HTL, HT and cHTG have an subsystem heat recovery of 80% each. Therefore, cold flows are not shown in the illustration. Significant quantities of heat are required for the HTL fuel production. The largest heat quantities are necessary in HTL (2.1 MJ kg^{-1} FS) and in cHTG (1.5 MJ kg^{-1} FS). The demand for electrical energy is much smaller, in total 0.6 MJ kg^{-1} FS without application of CHP are consumed. The electrical energy produced by CHP with 0.8 kJ kg^{-1} FS is sufficient to cover the demand of an HTL process chain. Therefore, no additional electric energy source is needed in an integrated HTL process chain. The computed energy flows in the energy balance form the basis for the implementation of an integrated heat management, which covers the entire HTL process chain and offers potential to increase process efficiency.

3.5. Heat exchangers

In order to minimize the heat demand, a HEN is developed comprising the entire HTL process chain considering an upgraded biocrude production of 10 kt per year. A list and a ranking regarding the heating or cooling duty of the cold and hot process streams serves as a basis for an optimal configuration and design of heat exchangers according to the pinch principles. To keep the process simple and to optimize costs with regard to the required heat exchanger surface area, only those streams were considered that have an enthalpy greater than 5 MJ per kg fuel. All considered hot and cold flows are listed in Table 4.

By identifying the pinch temperature and starting to design the heat transfer network around this point, the energy targets can be met by transferring heat between hot and cold flows. The arrangement of the heat exchangers and the required heat exchange surface is shown in Table 5.

The two heat exchangers comprising cHTG and HTL are of almost equal size and have a surface area of 1.71 and 1.69 m^2 respectively. The heat exchanger used to preheat the HTL slurry is slightly smaller with 1.01 m^2. A cumulated heat exchanger surface of 4.41 m^2 is computed. In Fig. 8 the cost optimization regarding the size of the heat exchanger surface area is illustrated related to a fuel production of 1 kg h^{-1}. The cost optimization minimizes the costs resulting from natural gas and electricity supply as well as the cost of the heat exchangers, as other cost parameters are assumed to be independent of the ratio of heat recovery.

The bends in the graphs at a heat exchanger area of 19.3 m^2 correspond to a condition where the complete heat demand of the process is covered from heat recovery. A further increase in heat exchanger area does not further improve the plant economics. Therfore, for a heat

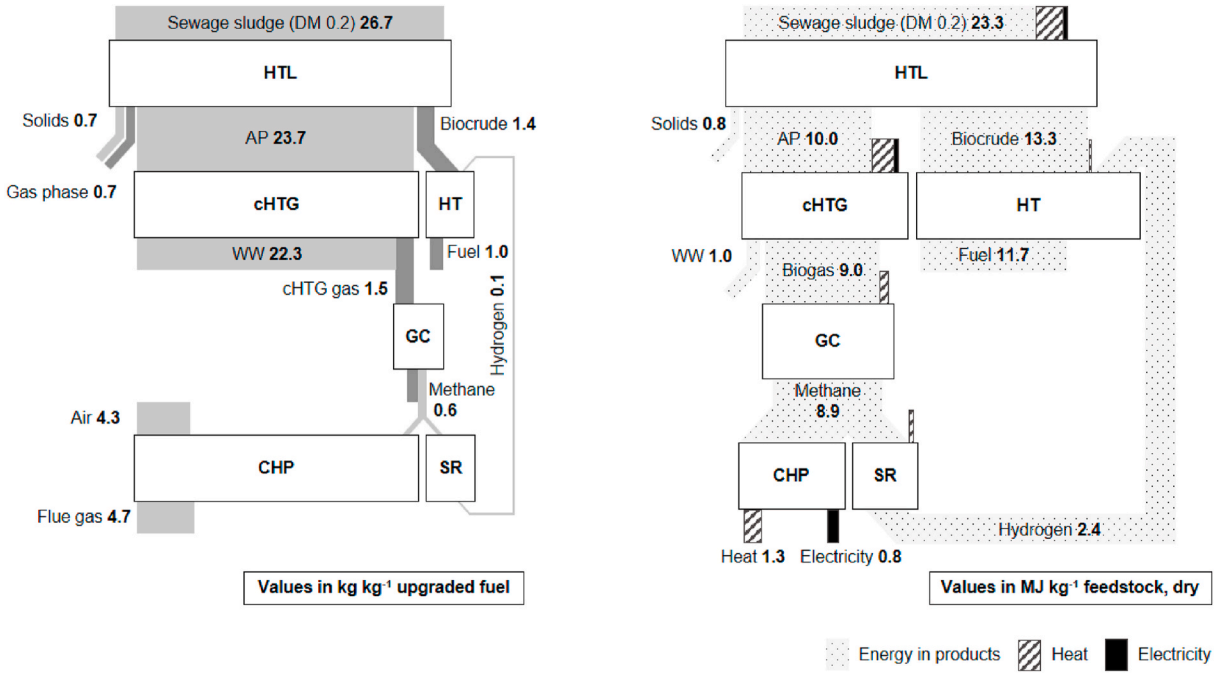

Fig. 7. Mass (left) and energy balance (right) for an HTL process chain using sewage sludge as HTL feed. (AP: aqueous phase; HTL: hydrothermal liquefaction; HT: hydrotreating; cHTG: catalytic hydrothermal liquefaction; GC: gas cleaning; CHP: combined heat and power plant; SR: steam reforming; WW: waste water).

Table 4
Input for the pinch analysis: List of considered hot and cold flows in an integrated HTL plant with their respective inlet and outlet temperatures and resulting enthalpy.

Name	Inlet T in °C	Outlet T in °C	Enthalpy in MJ kg^{-1}
HTL slurry in	25	350	35.22
HTL slurry out	350	80	29.26
cHTG in	80	450	29.48
cHTG out	450	80	29.48
CHP out	810	25	25.00

Table 5
Configuration of the modeled heat exchangers related to an upgraded biocrude production of 1 kg h^{-1}.

Stream in, hot	Stream in, cold	ΔT_{LM} in °C	Area in m^2
cHTG out	HTL slurry in	318	1.71
HTL slurry out	cHTG in	316	1.69
CHP out	HTL slurry in	151	1.01

exchanger surface area of 19.3 m^2 (related to a fuel production of 1 kg h^{-1}), the cost-optimized process configuration results.

3.6. Comparison of different process configurations

Fig. 9 summarizes the computed process efficiencies and considered production costs for different heat recovery options and HTL process configurations.

The first considered heat exchange configuration is referred to as "no heat recovery option" (No HR) in the following. In this configuration, the process streams are spatially connected between the individual process steps, but there is no heat exchange between hot and cold streams. The second heat recovery configuration describes heat exchangers that only comprise an individual process step. For example the heat exchanger of the HTL pilot plant at Aarhus University performs with a heat recovery of 80% [3]. For this consideration, it is assumed that in each high-temperature process step, individual heat recovery is

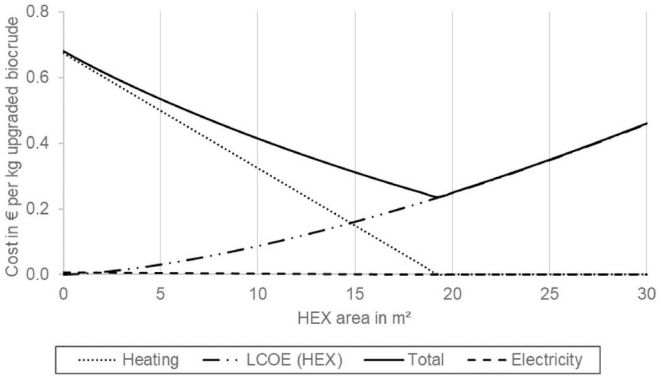

Fig. 8. Cost optimization for the heat recovery for processing sewage sludge via HTL related to an upgraded biocrude production of 1 kg h^{-1}. Costs for electricity are proportionately low. (HEX: heat exchanger; LCOE: levelized cost of energy).

performed with a heat recovery efficiency of 80%. The HEN, which includes an energetic optimization of the heat exchanger assembly and a cost optimization of the heat exchanger surface area, forms the third system configuration considered.

In addition, the process efficiency was determined for the following three process configurations: In the first process configuration, the HTL process is coupled with the upgrading step. The second process configuration is based on the first one, but additionally includes the energetic use of the aqueous phase by cHTG and CHP. Finally, a process configuration, in which a part of the methane produced by cHTG is used energetically by CHP and some of the methane is used for the production of the internally required hydrogen, is considered.

From the data it is clear that heat recovery within the HTL and cHTG subsystems is essential for all process configurations. The efficiency can be further improved by using an integrated HEN. For the first process configuration the heat exchanger network is not applicable, because in the HTL process no additional waste heat can be used for upgrading.

The overall best process efficiency with a value of 44.2% can be

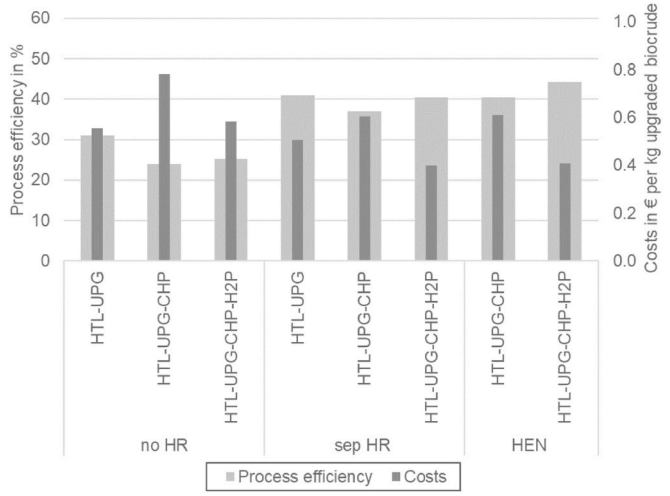

Fig. 9. Achievable process efficiencies and considered costs: no heat recovery (no HR), individual heat recovery in each process step (sep HR), heat exchanger network (HEN).

achieved with a process configuration in which an energetic use of the aqueous phase is carried out and hydrogen is produced on site. For the case of an external hydrogen supply and an application of a heat exchanger network, a process efficiency of 40.3% can be calculated. Since this configuration can be favorable from an economic or environmental point of view and the process efficiency is only slightly lower, this also offers a promising option as configuration of an HTL process chain.

In addition to process efficiency, the production cost items were compared. The lowest costs can be generated with an integrated HTL process chain (0.58 € for no HR, 0.40 € for SEP HR, 0.41 € for HEN). The options where no treatment of the AP by means of cHTG or no on-site hydrogen production is carried out are worse from a cost perspective.

Fig. 10 shows how the costs are composed for the most economical process configuration namely an integrated HTL fuel production chain with an on-site hydrogen generation and a separated heat recovery. Note that the chart shows only selected cost items associated with the investigated subsystems, further important cost contributions such as labor or gate fees for sewage sludge treatment are not considered here. In the here shown process configuration addditional hydrogen is not required and therefore not assossiated with costs.The cost for electrical energy takes a small share (1.3%). Most of the costs are due to methane (17.5%), which is used for heat supply, and the investment costs for biocrude production (21.9%) and heat exchangers (24.3%).

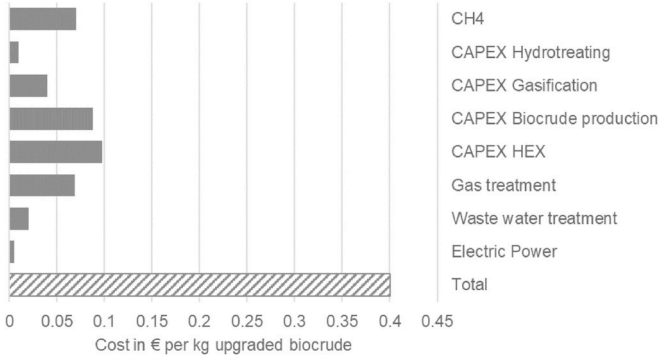

Fig. 10. Overview of considered cost items for a fuel production by HTL of sewage sludge. The cost optimized process configuration was considered (33% of methane used for hydrogen generation, separated HR).

4. Discussion

The field of HTL process models can be differentiated by several characteristics, two of them being the use of a reaction network and the consideration of a process chain connected to the HTL process. Previous studies of the HTL process including a reaction network are mainly based on HTL batch experiments. Most of these studies use a small number of model compounds and do not consider a process chain connected to the HTL process [40]. The most prominent system analyses of continuous HTL processes and process chains were performed by the Pacific Northwest National Laboratory [41]. However, in these publications no reaction network is considered and product yields and compositions are specified according to experimental results. In this work, all the above mentioned aspects are combined in a single process chain model. Furthermore, the considered process chain is analysed with respect to several different process configurations and heat recovery options. Based on the results, further considerations towards environmentally and economically favorable plant designs can be made.

4.1. Thermochemical modeling

One variable that can be used to validate a model with integrated reaction network is the elemental analysis. Some minor and moderate differences can be observed for the comparison of the three most important streams; feedstock, biocrude and upgraded biocrude. Generally, most of the relative deviations for all three streams are below 10%. Exceptions to this finding are the relative deviation of the nitrogen content in the biocrude as well as the relative deviations of the nitrogen and oxygen contents in the upgraded biocrude. The latter two are in the range of 40–44% for oxygen and nitrogen, respectively, and can be attributed to the very small absolute values.

Besides the distribution of elements in the three important streams, also the distribution of boiling points of components in the final product stream can serve as criterion for validation of the model (compare Fig. 5). It should be noted, that experimental results of the final boiling point distribution can vary significantly depending on the conditions during hydrotreatment and distillation. Moreover, the herein cited experimental results are not obtained from one continuously operated process chain, but from different individual experiments that are not directly associated with each other. Thus, the experimental results should rather be viewed as an indicator for the model, and not as strict empirical realities that have to be matched by the modeling. Considering this, the model results are in good agreement with the experimental results and the deviations are assumed to be in an acceptable range. The accuracy of the modeling can be improved further by an increased number of experimental data, especially in the context of continuously operated HTL process chains, and by the availability of thermodynamic data for a greater variety of representative compounds in the process streams.

4.2. Limitations for heat recovery

Intensive heat recovery can significantly increase the efficiency of a fully integrated HTL process. However, when designing a heat recovery system, certain limitations have to be taken into account. The main limitation in heat recovery is the phase separation in the process steps HTL, HT and cHTG. Product streams have to be cooled down to a temperature of about 80 °C in order to realize a sufficient separation of the product phases. Hereby, major hot-cold gradients lead to a decrease in overall efficiency. Since high temperatures (exceeding 500 °C in CHP flue gas) occur in the process, care has to be taken when selecting suitable materials for the implementation of a system. A further factor that has to be considered in the technical implementation of a HEN is the possibility of precipitation of mineral components during cooling of the product streams. With temperature decrease salts in the pipes or in the heat exchangers can precipitate, leading to an increased corrosion risk as

well as to a reduced heat exchange efficiency.In addition, limitations due to the specific HTL plant need be taken into account, when dimensioning a HEN. Heat exchangers may not be installed at every point in the system in the desired dimension. However, this can only be assessed when designing and dimensioning a plant in detail.

4.3. Further considerations for HTL plant design

The investigated plant layout, which includes subcritical HTL, cHTG for aqueous phase treatment and hydrotreating towards transportation fuel products like gasoline, diesel and jet fuel, represents a specific choice of subsystems, which is also investigated experimentally in the EU-project HyFlexFuel. Designing HTL plants for other purposes, e.g. for the production of biooils for the heating or marine sector, will also have an impact on plant design, especially regarding the upgrading process. Fig. 9 indicates that the results are most relevant for the thermal integration of the HTL and the cHTG step. However, further options for the treatment and energetic valorization of the aqueous phase, such as anaerobic digestion, do not require high temperatures and pose different challenges for process modeling and plant integration. HTL and aqueous phase treatment will likely be implemented at a common location. In contrast, for many HTL process chains transportation of biocrudes to centralized hydrotreatment plants, or co-feeding of HTL biocrudes in conventional refineries might be advantageous. The modeling results show only a small benefit of thermal integration of hydrotreatment at a common location. The generation of hydrogen from cHTG gas makes sense from an energy perspective, but hydrogen generation from other sources may still be more competitive at refineries and centralized upgrading plants. In both cases a HTL plant may still involve a limited partial upgrading step to improve the quality and stability of the biocrude, which is then transported to centralized facilities. Yet another option is the coupling of HTL process chains or subsystems of HTL process chains with other energy or waste management systems. Examples include the availability of additional heat sources, generation of renewable hydrogen via electrolysis, or sharing facilities for aqueous phase treatment.

5. Conclusions

The results indicate that an energetic valorization of the organic content in the aqueous phase can be beneficial for HTL plants, as a significant fraction of the organic content from the biomass feedstock is converted into soluble compounds, which separate from the biocrude. cHTG provides a potential option to convert the organics in the aqueous phase into a biogas and thereby also clean up the process water for environmentally sound disposal. A close thermal integration is in particular beneficial for the HTL and cHTG subsystems, as both process steps require to lift the large thermal mass of their aqueous feed streams to elevated process temperatures. Consequently, the HTL and cHTG subsystems require substantial amounts of heating and cooling for their operation. Hydrogen generation from cHTG gas for biocrude upgrading via hydrotreatment is another potential benefit from plant integration, while the potential for thermal integration of the upgrading step seems to be limited, as a comparably small stream of biocrude-oil is processed. The modelling results return an overall energy efficiency of 44.2% in case of thermal integration and onsite hydrogen and process energy generation from cHTG gas. The energy efficiency is lower, 40.3%, in case of external hydrogen supply. Further investigations are required to weigh the benefits of on-site integration of hydrotreating, against the advantages of centralized biocrude upgrading facilities with improved economy of scale, or co-processing of HTL biocrudes in refineries. The optimum configuration may differ depending on the capacity or the specific geographical context of the individual HTL plant, a potential integration of electrolysis hydrogen may once more revise design choices. The modeling lays the basis for techno-economic and environmental system analyses of integrated HTL plants for transportation fuel production from sewage sludge and various other organic feedstock.

Acknowledgements

This project has received funding from the European Union's Horizon 2020 research and innovation programme under grant agreement No. 764734.

Appendix A. Supplementary data

Supplementary data to this article can be found online at https://doi.org/10.1016/j.biombioe.2021.106123.

Appendix

Table A1
General chemical composition of biomass based on basic components, building blocks and model components.

Basic component	Building block	Model component
Lipids	Fatty acids	Oleic acid
		Palmitic acid
		Arachidic acid
		Behenic acid
	Glycerol	Glycerol
Carbohydrates	Glucose (Cellulose)	Glucose
	Xylose and other sugars (Hemicellulose)	Xylose
Proteins	Amino acids	3-Mercaptopropionic acid
		Glycine
		Glutamine
		Tryptophane
		Phenylalanin
		Lysine
		2-Ethylimidazol
		Pyrrolidine
		Formic Acid
		Valeric Acid
		Ammonia
Lignin	Benzene and derivates	Benzene
		Benzoic acid
	Phenylpropanoid derivates	Eugenol

(*continued on next page*)

Table A1 (*continued*)

Basic component	Building block	Model component
	Phenol and derivates	Phenol
		4-hydroxybenzaldehyde
		Catechol
		Guaiacol
		Orcin
Ash	Metal oxides and hydroxids	Calcium Oxide
		Potassium Oxide
		Magnesium Hydroxide
		Sodium Oxide
		Iron Oxide
	Phosphates	Ammoniumdihydroxyphosphate

References

[1] J. Ramirez, R. Brown, T. Rainey, A review of hydrothermal liquefaction bio-crude properties and prospects for upgrading to transportation fuels, Energies 8 (2015) 6765–6794, https://doi.org/10.3390/en8076765.

[2] D.C. Elliott, T.R. Hart, A.J. Schmidt, G.G. Neuenschwander, L.J. Rotness, M. V. Olarte, A.H. Zacher, K.O. Albrecht, R.T. Hallen, J.E. Holladay, Process development for hydrothermal liquefaction of algae feedstocks in a continuous-flow reactor, Algal Research 2 (2013) 445–454, https://doi.org/10.1016/j.algal.2013.08.005.

[3] K. Anastasakis, P. Biller, R. Madsen, M. Glasius, I. Johannsen, Continuous hydrothermal liquefaction of biomass in a novel pilot plant with heat recovery and hydraulic oscillation, Energies 11 (2018) 2695, https://doi.org/10.3390/en11102695.

[4] R.B. Madsen, M. Glasius, How do hydrothermal liquefaction conditions and feedstock type influence product distribution and elemental composition? Ind. Eng. Chem. Res. 58 (2019) 17583–17600, https://doi.org/10.1021/acs.iecr.9b02337.

[5] D.C. Elliott, P. Biller, A.B. Ross, A.J. Schmidt, S.B. Jones, Hydrothermal liquefaction of biomass: developments from batch to continuous process, Bioresour. Technol. 178 (2015) 147–156, https://doi.org/10.1016/j.biortech.2014.09.132.

[6] F. Goudriaan, D.G.R. Peferoen, Liquid fuels from biomass via a hydrothermal process, Chem. Eng. Sci. 45 (1990) 2729–2734, https://doi.org/10.1016/0009-2509(90)80164-A.

[7] R.P. Nielsen, G. Olofsson, E.G. Søgaard, CatLiq – high pressure and temperature catalytic conversion of biomass: the CatLiq technology in relation to other thermochemical conversion technologies, Biomass Bioenergy 39 (2012) 399–402, https://doi.org/10.1016/j.biombioe.2012.01.035.

[8] I.M. Sintamarean, I.F. Grigoras, C.U. Jensen, S.S. Toor, T.H. Pedersen, L. A. Rosendahl, Two-stage alkaline hydrothermal liquefaction of wood to biocrude in a continuous bench-scale system, Biomass Conv. Bioref. 7 (2017) 425–435, https://doi.org/10.1007/s13399-017-0247-9.

[9] J. Lane, The Silver in Silva: the Story of Steeper Energy and SGF's's $59M advanced biofuels project in Norway. https://www.biofuelsdigest.com/bdigest/2018/01/16/the-silver-in-silva-the-story-of-steeper-energys-59m-advanced-biofuels-project-in-norway/, 2018. (Accessed 6 August 2020).

[10] C.U. Jensen, J.K. Rodriguez Guerrero, S. Karatzos, G. Olofsson, S.B. Iversen, Fundamentals of Hydrofaction™: renewable crude oil from woody biomass, Biomass Conv. Bioref. 7 (2017) 495–509, https://doi.org/10.1007/s13399-017-0248-8.

[11] D. Castello, T. Pedersen, L. Rosendahl, Continuous hydrothermal liquefaction of biomass: a critical review, Energies 11 (2018) 3165, https://doi.org/10.3390/en11113165.

[12] M.N. Nabi, M.M. Rahman, M.A. Islam, F.M. Hossain, P. Brooks, W.N. Rowlands, J. Tulloch, Z.D. Ristovski, R.J. Brown, Fuel characterisation, engine performance, combustion and exhaust emissions with a new renewable Licella biofuel, Energy Convers. Manag. 96 (2015) 588–598, https://doi.org/10.1016/j.enconman.2015.02.085.

[13] B.B. Dani Morán, Muradel demonstration plant. https://biorrefineria.blogspot.com/2016/06/muradel-demonstration-plant-microalgae.html, 2016. (Accessed 20 October 2020).

[14] European Commision, Disposal and Recycling Routes for Sewage Sludge: Part 4 – Economic Report, 2002, ISBN 92-894-1801-X. Luxembourg.

[15] L.J. Snowden-Swan, J.M. Billing, M. Thorson, A. Schmidt, M. Santosa, S.B. Jones, R. Hallen, Wet Waste Hydrothermal Liquefaction and Biocrude Upgrading to Hydrocarbon Fuels: 2019 State of Technology: PNNL-29882. https://doi.org/10.2172/1415710.

[16] L.J. Snowden-Swan, Y. Zhu, M.J. Bearden, T.E. Seiple, J.M. Billing, R. Hallen, T. R. Hart, J. Liu, K.O. Albrecht, S.P. Fox, G.D. Maupin, D.C. Elliott, Conceptual biorefinery design and research targeted for 2022: hydrothermal liquefaction processing of wet waste to fuels. https://www.pnnl.gov/main/publications/external/technical_reports/PNNL-29882.pdf, 2017. (Accessed 26 April 2021).

[17] P. Biller, I. Johannsen, J.S. Dos Passos, L.D.M. Ottosen, Primary sewage sludge filtration using biomass filter aids and subsequent hydrothermal co-liquefaction, Water Res. 130 (2018) 58–68, https://doi.org/10.1016/j.watres.2017.11.048.

[18] D. López Barreiro, B.R. Gómez, F. Ronsse, U. Hornung, A. Kruse, W. Prins, Heterogeneous catalytic upgrading of biocrude oil produced by hydrothermal liquefaction of microalgae: state of the art and own experiments, Fuel Process. Technol. 148 (2016) 117–127, https://doi.org/10.1016/j.fuproc.2016.02.034.

[19] J.A. Arzate, M. Kirstein, F.C. Ertem, E. Kielhorn, H. Ramirez Malule, P. Neubauer, M.N. Cruz-Bournazou, S. Junne, Anaerobic digestion model (AM2) for the description of biogas processes at dynamic feedstock loading rates, Chem. Ing. Tech. 89 (2017) 686–695, https://doi.org/10.1002/cite.201600176.

[20] P.A. Marrone, D.C. Elliott, J.M. Billing, R.T. Hallen, T.R. Hart, P. Kadota, J. C. Moeller, M.A. Randel, A.J. Schmidt, Bench-scale evaluation of the genifuel hydrothermal processing technology for wastewater solids, in: Proceedings of the Water Environment Federation, 2017, https://doi.org/10.2175/193864717822157702.

[21] M.S. Haider, D. Castello, L.A. Rosendahl, Two-stage catalytic hydrotreatment of highly nitrogenous biocrude from continuous hydrothermal liquefaction: a rational design of the stabilization stage, Biomass Bioenergy 139 (2020) 105658, https://doi.org/10.1016/j.biombioe.2020.105658.

[22] B. Maddi, E. Panisko, T. Wietsma, T. Lemmon, M. Swita, K. Albrecht, D. Howe, Quantitative characterization of the aqueous fraction from hydrothermal liquefaction of algae, Biomass Bioenergy 93 (2016) 122–130, https://doi.org/10.1016/j.biombioe.2016.07.010.

[23] J. Reimer, G. Peng, S. Viereck, E. de Boni, J. Breinl, F. Vogel, A novel salt separator for the supercritical water gasification of biomass, J. Supercrit. Fluids 117 (2016) 113–121, https://doi.org/10.1016/j.supflu.2016.06.009.

[24] HyFlexFuel, Hydrothermal liquefaction: enhanced performance and feedstock flexibility for efficient biofuel production; Grant agreement No. 764734. https://cordis.europa.eu/project/id/764734/de, 2017 accessed 26 April 2021.

[25] C. Penke, L. Moser, V. Batteiger, Modelling of cost optimized HTL fuel production by process integration, in: 8th European Biomass Conference & Exhibition, e-EUBCE, Marseille, France (virtual event), 2020, https://doi.org/10.5281/zenodo.4314750.

[26] L.B. Silva Thomsen, P.N. Carvalho, J.S. Dos Passos, K. Anastasakis, K. Bester, P. Biller, Hydrothermal liquefaction of sewage sludge; energy considerations and fate of micropollutants during pilot scale processing, Water Res. 183 (2020) 116101, https://doi.org/10.1016/j.watres.2020.116101.

[27] T. Horschig, C. Penke, A. Habersetzer, V. Batteiger, HyFlexFuel Public report: regional feedstock potentials and preference regions for HTL projects. https://ec.europa.eu/research/participants/documents/downloadPublic?documentIds=080166e5ca952590&appId=PPGMS, 2020. (Accessed 26 April 2021).

[28] J. Yang, Q. He, H. Niu, K. Corscadden, T. Astatkie, Hydrothermal liquefaction of biomass model components for product yield prediction and reaction pathways exploration, Appl. Energy 228 (2018) 1618–1628, https://doi.org/10.1016/j.apenergy.2018.06.142.

[29] A.A. Shah, S.S. Toor, T.H. Seehar, R.S. Nielsen, A.H. Nielsen, T.H. Pedersen, L. A. Rosendahl, Bio-Crude production through aqueous phase recycling of hydrothermal liquefaction of sewage sludge, Energies 13 (2020) 493, https://doi.org/10.3390/en13020493.

[30] J.J. Ortega-Calvo, C. Mazuelos, B. Hermosin, C. Saiz-Jimenez, Chemical composition of Spirulina and eukaryotic algae marketed in Spain, J. Appl. Phycol. 5 (1993) 425–435, 1993, https://link.springer.com/article/10.1007/BF02182735. (Accessed 26 April 2021).

[31] E. Lappa, P.S. Christensen, M. Klemmer, J. Becker, B.B. Iversen, Hydrothermal liquefaction of miscanthus × giganteus: preparation of the ideal feedstock, Biomass Bioenergy 87 (2016) 17–25, https://doi.org/10.1016/j.biombioe.2016.02.008.

[32] Y. Zhu, S.B. Jones, A.J. Schmidt, K.O. Albrecht, S.J. Edmundson, D.B. Anderson, Techno-economic analysis of alternative aqueous phase treatment methods for microalgae hydrothermal liquefaction and biocrude upgrading system, Algal Research 39 (2019) 101467, https://doi.org/10.1016/j.algal.2019.101467.

[33] N. Boukis, E. Hauer, S. Herbig, J. Sauer, F. Vogel, Catalytic gasification of digestate sludge in supercritical water on the pilot plant scale, Biomass Conv. Bioref. 7 (2017) 415–424, https://doi.org/10.1007/s13399-017-0238-x.

[34] D. Castello, M.S. Haider, L.A. Rosendahl, Catalytic upgrading of hydrothermal liquefaction biocrudes: different challenges for different feedstocks, Renew. Energy 141 (2019) 420–430, https://doi.org/10.1016/j.renene.2019.04.003.

[35] K.F. Tzanetis, J.A. Posada, A. Ramirez, Analysis of biomass hydrothermal liquefaction and biocrude-oil upgrading for renewable jet fuel production: the

impact of reaction conditions on production costs and GHG emissions performance, Renew. Energy 113 (2017) 1388–1398, https://doi.org/10.1016/j.renene.2017.06.104.
[36] S. Li, Y. Jiang, L.J. Snowden-Swan, J.A. Askander, A.J. Schmidt, J.M. Billing, Techno-economic uncertainty analysis of wet waste-to-biocrude via hydrothermal liquefaction, Appl. Energy 283 (2021) 116340, https://doi.org/10.1016/j.apenergy.2020.116340.
[37] S. Keshavarzian, V. Verda, E. Colombo, P. Razmjoo, Fuel saving due to pinch analysis and heat recovery in a petrochemical company, in: 28th International Conference on Efficiency, Cost, Optimization, Simulation and Environmental Impact of Energy Systems, ECOS, France, 2015, https://doi.org/10.13140/RG.2.1.3099.7603.
[38] T. Milne, A.H. Brennan, B.H. Glenn, in: Sourcebook of Methods of Analysis for Biomass and Biomass Conversion Processes, first ed., Springer, Netherlands, 1990, ISBN 978-1-85166-527-3.
[39] J.M. Jarvis, K.O. Albrecht, J.M. Billing, A.J. Schmidt, R.T. Hallen, T.M. Schaub, Assessment of hydrotreatment for hydrothermal liquefaction biocrudes from sewage sludge, microalgae, and pine feedstocks, Energy Fuels 32 (2018) 8483–8493, https://doi.org/10.1021/acs.energyfuels.8b01445.
[40] J. Hoffmann, S. Rudra, S.S. Toor, J.B. Holm-Nielsen, L.A. Rosendahl, Conceptual design of an integrated hydrothermal liquefaction and biogas plant for sustainable bioenergy production, Bioresour. Technol. 129 (2013) 402–410, https://doi.org/10.1016/j.biortech.2012.11.051.
[41] Y. Zhu, M.J. Biddy, S.B. Jones, D.C. Elliott, A.J. Schmidt, Techno-economic analysis of liquid fuel production from woody biomass via hydrothermal liquefaction (HTL) and upgrading, Appl. Energy 129 (2014) 384–394, https://doi.org/10.1016/j.apenergy.2014.03.053.
[42] P. Hein, F. Peter, P. Graichen, in: The German Power Market: State of Affairs, 2019. https://www.agora-energiewende.de/en/publications/the-german-power-market-state-of-affairs-in-2019/. (Accessed 29 April 2021).
[43] Stadtwerke Esslingen, Neue Wasserpreise und Abwassergebühren zum 1, Januar (2019), 2018, https://www.swe.de/de/News-room/Aktuelles/Pressemeldung-20181/Neue-Wasserpreise-und-Abwassergebuehren-zum-1.-Januar-2019-.html. (Accessed 2 July 2020).
[44] Biogasnetzeinspeisung, Vergleich der Verfahren zur Methananreicherung. https://www.biogas-netzeinspeisung.at/technische-planung/aufbereitung/methananreicherung/vergleich-verfahren.html, 2014. (Accessed 2 July 2020).
[45] B.L. Capehart, Microturbines | WBDG - whole building design guide. https://www.wbdg.org/resources/microturbines, 2020. (Accessed 4 November 2020), 982Z.
[46] Eurostat, Gas prices for non-household consumers - bi-annual data (from 2007 onwards). https://ec.europa.eu/eurostat/databrowser/view/nrg_pc_203/default/table?lang=en, 2021. (Accessed 29 April 2021).

Abbreviations

AP: Aqueous phase
daf: Dry and ash free
DM: Dry matter
CAPEX: Capital expenditure
CHP: Combined heat and power plant
cHTG: Catalytic hydrothermal gasification
EA: Elementary analysis
FS: Feedstock
GC: Gas cleaning
H2P: Hydrogen production
HEN: Heat exchange network
HEX: Heat exchanger
HR: Heat recovery
HT: Hydrotreating
HTL: Hydrothermal liquefaction
HTU: Hydrothermal upgrading
LCOE: Levelized cost of energy
PNNL: Pacific Northwest National Laboratory
PR-BM: Peng-Robinson equation of state with Boston-Mathias modification
PV: Present Value
REQUIL: Equilibrium reactor model
RGIBBS: Gibbs reactor model
RSTOIC: Stoichiometric reactor model
SEP: Separator
SR: Steam reforming
STHR: Steam heater
TEA: Techno-economic assessment
UPG: Upgrading process
WW: Waste water